

Received February 24, 2020, accepted March 9, 2020, date of publication March 16, 2020, date of current version March 27, 2020.

Digital Object Identifier 10.1109/ACCESS.2020.2980932

Design of a Miniaturized Printed Multi-Turn Loop Antenna for Shielding Effectiveness Measurement

EUNJUNG KANG¹, TAE HEUNG LIM¹, SANGWOON YOUN¹, DAE HEON LEE²,
KI BAEK KIM², AND HOSUNG CHOO¹, (Senior Member, IEEE)

¹School of Electronic and Electrical Engineering, Hongik University, Seoul 04066, South Korea

²Electronics and Telecommunications Research Institute, Daejeon 34044, South Korea

Corresponding author: Hosung Choo (hschoo@hongik.ac.kr)

This article is a result that was implemented as a research project by affiliated Institute of ETRI.

ABSTRACT This paper proposes a novel miniaturized loop antenna consisting of a multi-turn printed strip and a ring-shaped ferrite core. The lateral surface of the ferrite core is tightly wrapped by the circular multi-turn strip, which is printed on a thin, ring-shaped Styrofoam. To verify the feasibility, the proposed antenna is fabricated, and the antenna factor (AF) levels are measured using the three-antenna method from the VLF to HF band. The AF levels by measurement, theory, and simulation are 36.14 dB, 34.01 dB, and 33.6 dB at 30 kHz, respectively. In the VLF band, the antenna has a diameter of 114 mm, which is miniaturized to less than 60% compared to previous research. In addition, the proposed antenna is employed in the shielding effectiveness (SE) measurement of a small commercial cabinet to observe its suitability for SE measurement of small shielding enclosures. The SE values averaged over the frequency range from 10 kHz to 3 MHz are 5.19 dB and 14.14 dB in the horizontal and vertical polarizations.

INDEX TERMS VLF antenna, ferrite loop antenna, multi-turn loop antenna, miniaturization, AF enhancement, SE measurement.

I. INTRODUCTION

Loop antennas are extensively used in the kHz to Terahertz frequency bands in a variety of applications, such as mobile communications, wireless power transfer, medical RF devices, and electromagnetic field (EMF) measurement equipment [1]–[7]. In particular, for very low frequencies of a few kHz, loop antennas are predominantly chosen as magnetic probes to measure the shielding effectiveness (SE) of various types of shielding enclosures. Recently, there has been a growing demand for small shielding enclosures to protect just electronic equipment to ensure lower maintenance costs than shielding entire systems. However, in the very low frequency (VLF) band, where the size and weight of the loop antenna must be significantly increased, it is almost impossible to measure the SE of such small shielding enclosures. Thus, many miniaturization techniques of loop antennas have been carried out to date, including, for example, using printed circuit boards [8], [9], employing a ceramic material [10], and adding lumped elements [11]. Although these approaches have been successful in reducing

physical antenna size to some extent, such techniques generally require complicated structures or expensive fabrication processes. In addition, the high antenna factor (AF) of these miniaturized loop antennas in the VLF band often results in inaccurate magnetic field measurements. To overcome these issues, there has been a tremendous effort to improve the accuracy of magnetic field measurement. Various loop antennas have been introduced, including a shielded conducting surface [12]–[14], applying two-port excitation [15]–[17], adding a parasitic loop element [18]–[20], and using a Moebius loop structure [21]–[23]. However, such previous studies have generally focused on improving measurement accuracy in the high frequency (HF) band, and an in-depth study on the miniaturization of loop antennas in the VLF band, which can maintain low AF levels, has not yet been carried out.

In this paper, we propose a miniaturized circular loop antenna with a novel design structure consisting of a multi-turn printed strip and a ring-shaped ferrite core. The circular multi-turn strip is printed on a thin, ring-shaped Styrofoam to tightly wrap the lateral surface of the ferrite core, which can maximize the number of strip turns. The center of the ferrite core is perforated inside and remained empty in order to considerably reduce the weight of the antenna

The associate editor coordinating the review of this manuscript and approving it for publication was Haiwen Liu.

for SE measurements in the VLF band. In the VLF band, the antenna has a diameter of 114 mm, which is miniaturized to less than 60% compared to previous research with diameters between 200 mm to 2000 mm [12], [15], [16]. The proposed design is modeled and simulated using the FEKO EM simulator [24] to observe the antenna characteristics and to compare them with the theoretical results. To verify the results, the proposed antenna is fabricated, and the AF levels are measured using the three-antenna method [25] from the VLF to HF band. We then observe the AF levels in accordance with the variations of the important antenna geometry parameters to better understand the operating principle. Finally, the proposed antenna is employed in the SE measurement of a small commercial cabinet. The results demonstrate that the proposed compact antenna with low AF levels is applicable for measuring the SE of small shielding enclosures in the VLF band.

II. ANTENNA GEOMETRY AND THEORY

A. GEOMETRY

Fig. 1 shows the geometry of the proposed antenna that is composed of a ring shape ferrite core ($\mu_r = 1800$ less than 100 kHz) and a circular printed multi-turn loop. The ring shape ferrite core has a diameter d_1 , and the inner hole of ferrite has a diameter d_2 with a height of h to reduce the weight of the antenna for easier movement of the antenna position in the SE measurement setup. The circular multi-turn strip with a diameter d_3 is printed on a thin ring-shaped

Styrofoam, which can maximize the turn number N_t . The strip has a width w and a pitch p between the adjacent strip. The ferrite core structure and the multi-turn loop can concentrate high magnetic flux density at the center of the antenna, and at the same time, the antenna diameter can be miniaturized to be less than 0.25 m in order to measure a small shielding enclosure usually having one side length of 0.75 m. The ends of the multi-turn strip are directly fed by a single N-type connector, and the detailed values of the design parameters are listed in Table 1. Figs. 2(a) to 2(c) present photographs of a fabricated antenna with a case cover. A Styrofoam is fabricated to be a ring-shaped structure by drilling the center of a circular Styrofoam. 5 mm wide multi-turn strips (made of copper tape) are cut to have a correct pitch spacing (2 mm), and attached onto the Styrofoam. The Styrofoam with the copper tape is wrapped around the ferrite core, and the ends of the copper tape are soldered to provide electrical connection.

TABLE 1. Design parameters of the proposed antenna.

Parameters	Values
d_1	104 mm
d_2	80 mm
d_3	114 mm
p	2 mm
w	5 mm
h	40 mm.
N_t	6

To enhance durability, a cylindrical acrylic jig is placed inside the case cover, which can hold the proposed antenna in the middle of the case. In addition, an N-type connector case is placed at the bottom of the case cover to make a direct feeding connection with the multi-turn loop, which can also be used as a handle for the SE measurements. This case cover allows the antenna to be stably fixed with little impact on antenna performance.

B. AF MEASUREMENT

Fig. 3(a) presents a conceptual figure of the multi-turn wire loop antenna for the receiving mode, where the antenna has a loop radius a and a wire radius b . The center of the multi-turn loop antenna is located at the origin, and the incident electromagnetic waves toward the antenna have a tilted angle ψ in the plane of incidence and θ along the z -axis. When the plane wave impinges upon the loop antenna, an open-circuit voltage (V_{oc}), as written in the equation (1), is induced between the output terminals 1 and 2 [24].

$$\begin{aligned}
 V_{oc} &= j\omega\pi a^2 B_z N_t \\
 &= j\omega\pi a^2 (\mu_0 H \cos \psi \sin \theta) N_t,
 \end{aligned}
 \tag{1}$$

where B_z is the incident magnetic flux density, and N_t is the number of turns for the loop antenna. μ_0 is the permeability in free space, and ω is the angular velocity of the wave. To calculate the V_{oc} , we assume the parameters H , ψ , and

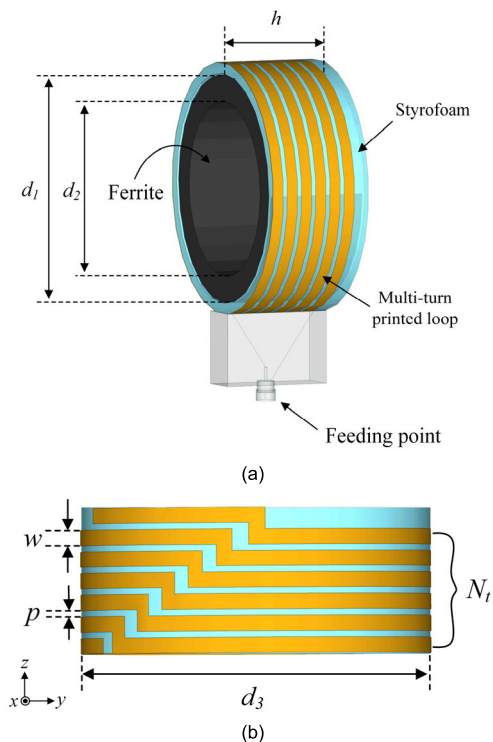


FIGURE 1. Geometry of the proposed antenna. (a) Isometric view. (b) Top view.

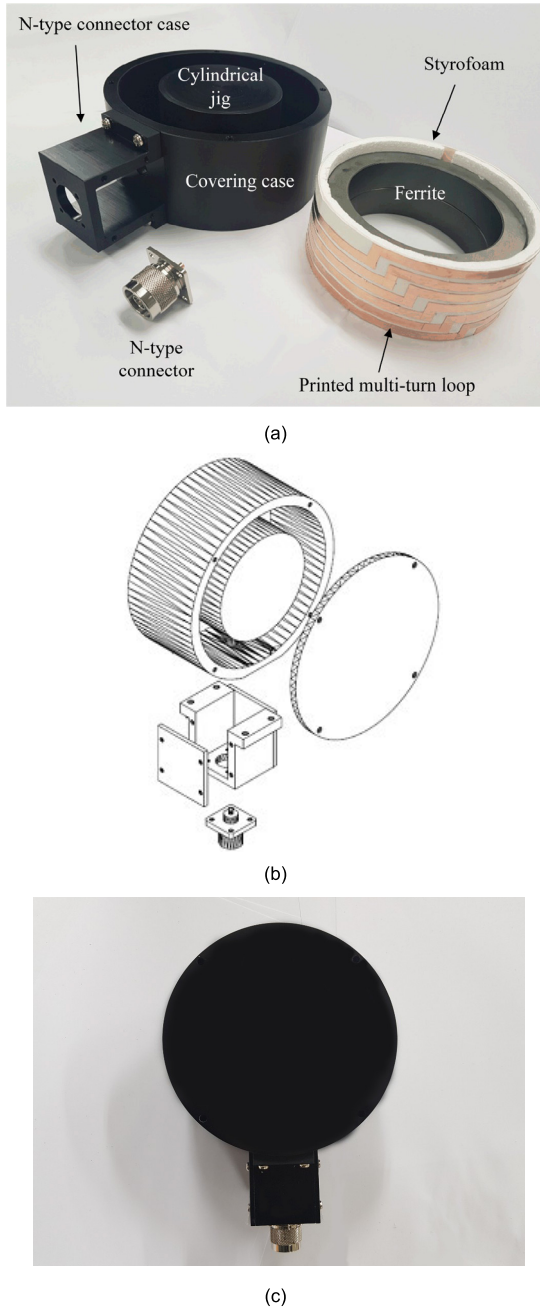


FIGURE 2. Photographs of the fabricated antenna. (a) Antenna parts. (b) Assembly process. (c) Assembled antenna.

θ set to be 1 A/m , 0° , and 90° , respectively. Fig. 3(b) presents a Thevenin equivalent circuit for the loop antenna with the open-circuit voltage. Z_L is a load impedance of 50Ω , and Z_{in} is the input impedance of the multi-turn loop antenna. From the voltage ratio theorem, we can obtain the V_L as derived in (2). Then, we can derive the theoretical AF (AF_{th}) of the receiving loop antenna from the following equation (3) [26].

$$V_L = V_{oc} \frac{Z_L}{Z'_{in} + Z_L}, \quad (2)$$

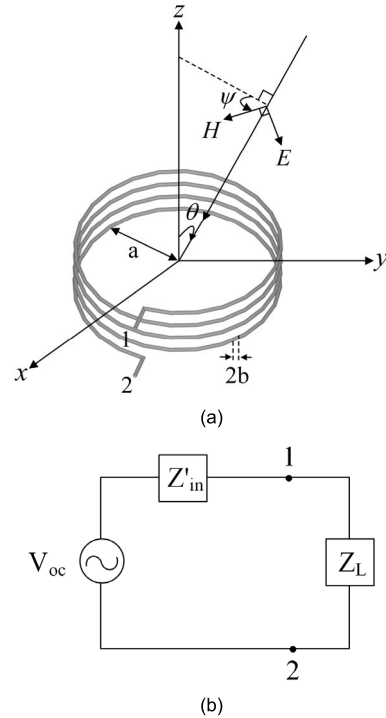


FIGURE 3. A conceptual figure of the multi-turn wire loop antenna for the receiving mode. (a) Plane wave incident toward the receiving loop. (b) Thevenin equivalent circuit model of the receiving loop antenna.

$$AF_{th} = \frac{H}{V_L}. \quad (3)$$

In addition, the AF characteristics of the proposed antenna are examined using the FEKO full EM software for comparison with the theoretical results. To obtain the AF levels for the proposed antenna, a plane wave source with 1 V/m and a load impedance Z_L of 50Ω are applied to the antenna to examine the magnetic field strength H and the induced voltage V_L across Z_L . H and V_L are obtained within the frequency range from 30 kHz to 20 MHz .

In the AF measurement, it is generally difficult to measure the exact magnetic field intensity, so we alternatively apply the three-antenna method to examine the AF levels. Fig. 4 illustrates the conceptual figure of the three-antenna method. In this method, two reference antennas and one test antenna are utilized to obtain S-parameters between Ant. 1 and Ant. 2 as well as Ant. 1 and Ant. 3 [14]. Then, the AFs for the three antennas can be defined as follows:

$$R_{pq} = \sqrt{d_{pq}^2 + r_p^2 + r_q^2}, \quad (4)$$

$$\alpha_{pq} = \frac{\sqrt{1 + k^2 R_{pq}^2}}{j2\pi f \mu_0 \pi Z_0 R_{pq}^3} \left\{ 1 + \frac{15(r_p r_q)^2}{8R_{pq}^4} + \frac{315(r_p r_q)^4}{64R_{pq}^8} + \dots \right\}, \quad (5)$$

$$AF_i = \left| \sqrt{\frac{-S_{nl} \alpha_{in} \alpha_{li}}{S_{in} S_{li} \alpha_{nl}}} \right|, \quad (6)$$

where d_{pq} is the distance between two testing antennas, and r_p and r_q are the radii of the loop antennas. k is the wavenumber

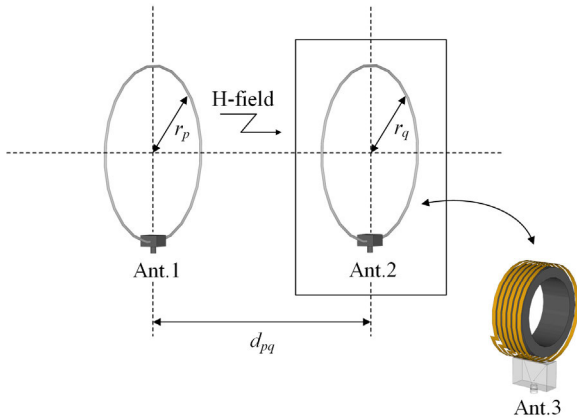


FIGURE 4. A conceptual figure of the three-antenna method for the AF measurement of the proposed antenna.

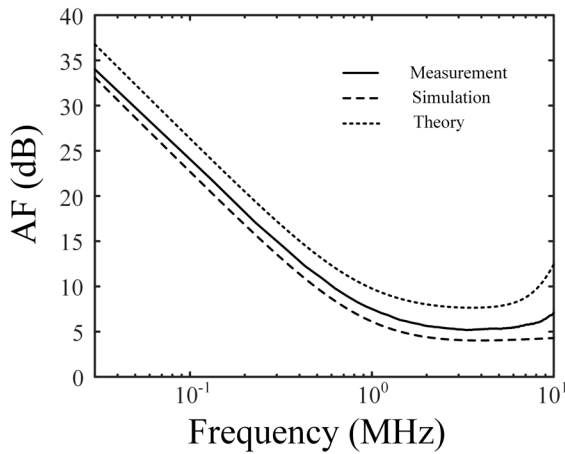


FIGURE 5. AF comparisons of the theory, simulation, and measurement.

in free space, and i , l , and n indicate the number of antenna indices. S_{nl} , S_{in} , and S_{li} are the S-parameters among the loop antennas, and f is the frequency of the measurement. Ant. 1 and Ant. 2 are two reference loop antennas with the same diameter of 300 mm, and Ant. 3 is the proposed antenna under the test. Then, the two loop antennas are placed at a distance d_{pq} of 240 mm. Then, the S_{12} and S_{13} are measured at 201 data points using the HP3753D network analyzer over the 30 kHz to 20 MHz. AF_3 in (6), obtained by this AF measurement setup, is the AF for the proposed antenna, and this value is compared with the theoretical and simulated AFs.

Fig. 5 presents the AF comparisons in terms of frequency. The AF levels of theory, simulation, and measurement are 36.14 dB, 34.01 dB, and 33.6 dB at 30 kHz, respectively. These AF levels are similar to 34 dB of the commercial loop antenna (SAS-563B from A.H. Systems) that has an even larger diameter of 30 cm. As the frequency increases, the AF does not improve after 30 MHz. This is because the multi-turn shape causes resonance, which rapidly increases the impedance, resulting in impedance mismatch. Fig. 6 shows the effect of the ferrite core on the AF. The AF

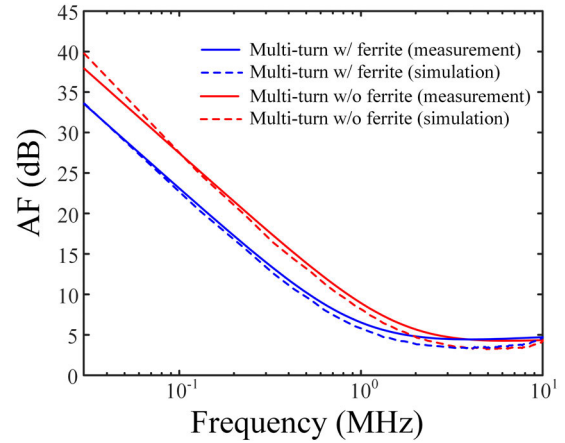


FIGURE 6. AF with and without the ferrite core.

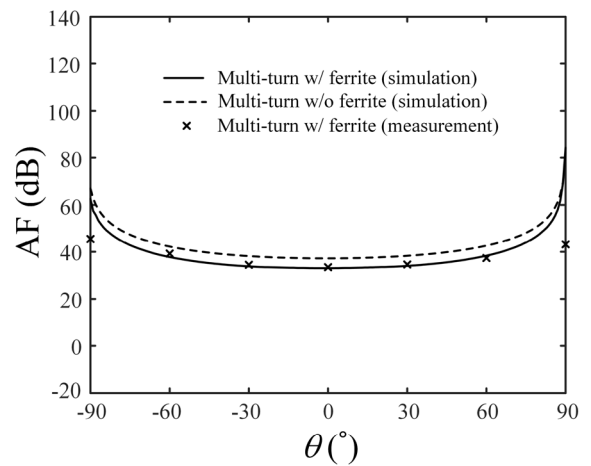


FIGURE 7. AF Comparisons between the simulation and measurement according to θ .

level with the ferrite core is 4.3 dB lower than without the ferrite core at 30 kHz. This result demonstrates that the AF level in the low-end frequency band can be decreased using the ferrite core. We also compare the properties between the proposed antenna and four reference commercial loop antennas. In this comparison, we examine the operating frequency, diameter, weight, and the AF levels at 30 kHz. The detailed explanations are given in Table 2.

Fig. 7 illustrates the simulation and measurement of the AFs according to the variation in the incident angle θ of the incident plane wave. When the incident plane wave encounters the proposed antenna at 60° , the simulated and measured results are 38.3 dB and 37.3 dB. As shown in the results, the proposed antenna can achieve stable AF levels despite incident angle variation ($-60 \leq \theta \leq 60$).

III. ANTENNA ANALYSIS AND SE MEASUREMENT

A. ANALYSIS

Fig. 8 presents the AF levels at the VLF band (10 kHz) in accordance with the variation in the antenna parameters N , l

TABLE 2. Antenna property comparisons.

	ETS-Lindgren (6512)	TDK (LP-0930P)	A.H.Systemes (SAS-563B)	Proposed
Operating frequency	9 kHz~30MHz	9 kHz~30MHz	10 kHz~30MHz	10 kHz~30MHz
Diameter (mm)	598	600	300	114
Weight (kg)	1.6	0.68	1.4	0.66
AF (dB) @ 30 kHz	7	21	16	33.6

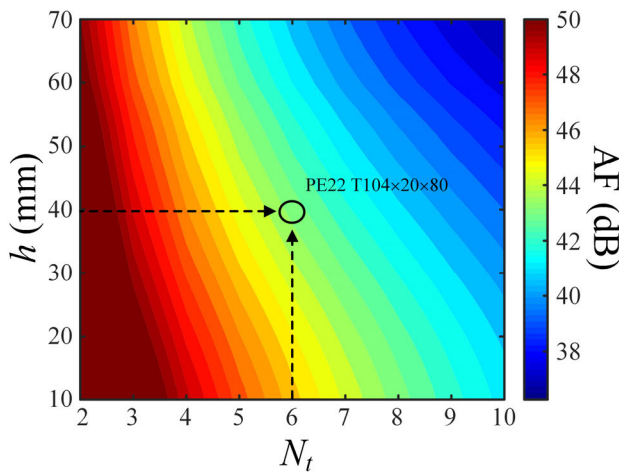
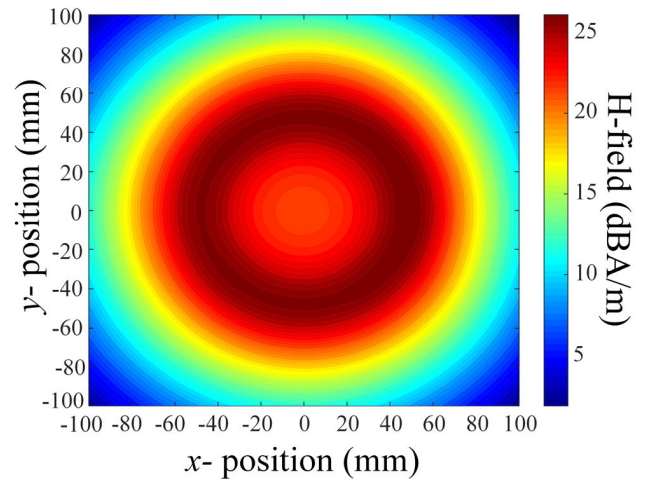
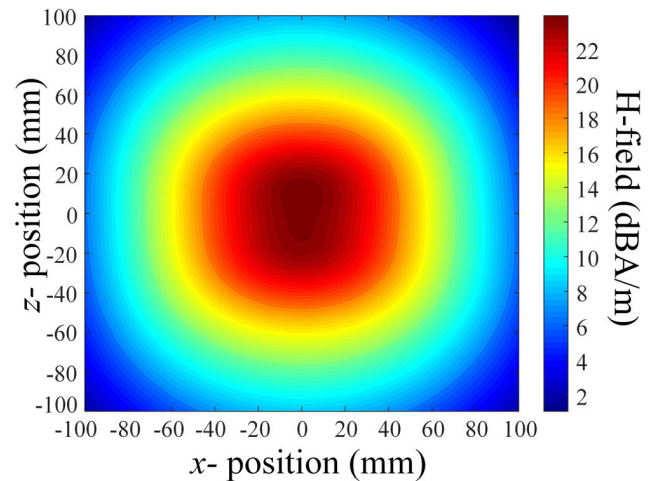


FIGURE 8. at low-end frequency in accordance with the variation of h and N_t .

and h . Lower AF levels can be observed when the turn number of the strip and the ferrite core height both gradually increase. Herein, although the lowest AF level cannot be achieved, the height h of the ferrite core is restricted to measure the SE in the small shielding enclosure. To reduce the size and weight of the proposed antenna, we use the ring-shaped ferrite core (PE22 T104 × 20 × 80 from TDK). The outer diameter of the ferrite is chosen to meet the SE measurement for small shielding enclosures with one side length less 0.75m as in the IEEE std 299.1. For the SE measurement of these enclosures, the outer diameter of the antenna should be less than 250 mm, and the antenna weight should also be considered. Therefore, the ring-shaped design with the inner diameter d_1 less than 250 mm is used. d_2 of 80 mm is used since it can reduce the weight from 1.4 kg ($d_2 = 0$ mm) to 1 kg ($d_2 = 80$ mm). The strip turn number N_t is also maximized within the ferrite core height h . These parameters are sensitively related to the AF levels, because N_t is relevant to concentrate the magnetic field, and h is related to the induced voltage.



(a)



(b)

FIGURE 9. H-field distributions. (a) xy -plane, (b) zx -plane.

Figs. 9(a) and 9(b) illustrate the H-field distributions around the proposed antenna in the xy - and zx -planes at 30 kHz when an input power of the antenna is 1 W. The



FIGURE 10. SE measurement setup using the proposed antenna.

magnetic near-field distributions are obtained in a volume of $-100 \text{ mm} \leq x, y, \text{ and } z \leq 100 \text{ mm}$ with $101 \times 121 \times 101$ sampling points. It can be seen that there are relatively strong magnetic fields in the center of the proposed antenna due to the ring-shaped ferrite core and multi-turn loop. Thus, such the ferrite core structure, as well as the multi-turn loop, allow to have low AF levels with the miniaturized antenna size in the VLF band.

B. SE MEASUREMENT

To verify that the proposed antenna is suitable for SE measurements, we carry out SE measurements for a small shielding enclosure from the VLF to the MF band based on IEEE standard 299.1 [27]. Fig. 10 presents a photograph of the SE measurement setup using the proposed antenna, including both the transmitting and receiving settings. The transmitting antenna (Tx) is connected to a function generator (DG 2041A from ROGOL) for transmitting a signal with a voltage of $10 V_{p-p}$ at the selected frequency (10 kHz to 3 MHz). Then, the receiving antenna (Rx) is connected to the spectrum analyzer (MS2720T from Anritsu) via a power amplifier with a gain of 18 dB. The Rx and Tx are separated by 0.3 m from the door of the small shielding enclosure. From this measurement setup, the SE can be calculated as follows:

$$SE = 20 \log_{10} \left| \frac{V_1}{V_2} \right| \quad (7)$$

where V_1 and V_2 denote received voltages when the receiving antenna is in free space and in the shielding enclosure, respectively. Fig. 11 shows the SE measurements in terms of the horizontal and vertical polarizations in the frequency range of 10 kHz to 3 MHz. The SE levels averaged over the entire

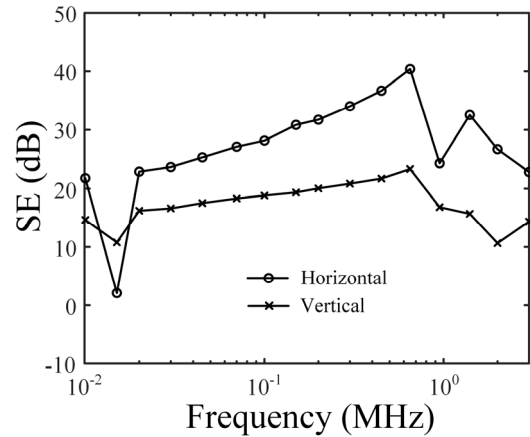


FIGURE 11. The measured SE in horizontal and vertical polarizations.

frequency range are 5.19 dB and 14.14 dB in the horizontal and vertical polarizations, respectively.

IV. CONCLUSION

The miniaturized circular loop antenna was proposed with a novel design approach consisting of the multi-turn printed strip and a ring-shaped ferrite core. The circular multi-turn strip was printed on the thin, ring-shaped Styrofoam to tightly wrap around the lateral surface of the ferrite core. Then, the proposed antenna was fabricated, and AF levels were measured from the VLF to the HF band to allow for comparison with the simulation and theoretical results. The AF levels of the theory, simulation, and measurement were 36.14 dB, 34.01 dB, and 33.6 dB at 30 kHz, respectively. In addition, we measured AF levels according to the variation in the incident angle of the plane wave. The simulated and measured results were 38.3 dB and 37.3 dB when the incident angle is 60° . Finally, the SE measurements were conducted in terms of the horizontal and vertical polarizations in the frequency range from 10 kHz to 3 MHz. The SE values averaged over the entire frequency range were 5.19 dB and 14.14 dB in the horizontal and vertical polarizations. These results demonstrated that the compact proposed antenna could be applicable in measuring the SE of small shielding enclosures in the VLF band.

REFERENCES

- [1] Q. Chen, K. Ozawa, Q. Yuan, and K. Sawaya, "Antenna characterization for wireless power-transmission system using near-field coupling," *IEEE Antennas Propag. Mag.*, vol. 54, no. 4, pp. 108–116, Aug. 2012.
- [2] B. B. Tierney and A. Grbic, "Planar shielded-loop resonators," *IEEE Trans. Antennas Propag.*, vol. 62, no. 6, pp. 3310–3320, Jun. 2014.
- [3] S. Curto and M. J. Ammann, "Circular loop antenna operating at 434 MHz for medical applications: Loop-tissue interaction," in *Proc. IET Irish Signals Syst. Conf. (ISSC)*, Aug. 2012, vol. 54, no. 4, pp. 108–116.
- [4] K. D. Katsibas, C. A. Balanis, P. A. Tirkas, and C. R. Birtcher, "Folded loop antenna for mobile hand-held units," *IEEE Trans. Antennas Propag.*, vol. 46, no. 2, pp. 260–266, Feb. 1998.
- [5] I. Yokoshima, "Absolute measurements for small loop antennas for RF magnetic field standards," *IEEE Trans. Instrum. Meas.*, vol. 23, no. 3, pp. 217–221, Sep. 1974.

- [6] S. Kim and H. Shin, "An ultra-wideband conformal meandered loop antenna for wireless capsule endoscopy," *J. Electromagn. Eng. Sci.*, vol. 19, no. 2, pp. 101–106, Apr. 2019.
- [7] Z. Zahid, L. Qu, H.-H. Kim, and H. Kim, "Circularly polarized loop-type ground radiation antenna for IoT applications," *J. Electromagn. Eng. Sci.*, vol. 19, no. 3, pp. 153–158, Jul. 2019.
- [8] S.-Y. Lin, S.-K. Yen, W.-S. Chen, and P.-H. Cheng, "Printed magnetic field probe with enhanced performances," in *Proc. Asia Pacific Microw. Conf.*, Dec. 2009, pp. 649–652.
- [9] Z. Yan, J. Luo, W. Zhang, Y. Wang, and J. Fan, "A simple miniature ultra-wideband magnetic field probe design for magnetic near-field measurements," *IEEE Trans. Antennas Propag.*, vol. 64, no. 12, pp. 5459–5465, Dec. 2016.
- [10] Y.-T. Chou and H.-C. Lu, "Electric field coupling suppression using via fences for magnetic near-field shielded-loop coil probes in low temperature co-fired ceramics," in *Proc. IEEE Int. Symp. Electromagn. Compat.*, Aug. 2011, pp. 6–10.
- [11] Y. Xia, J. Luo, and H. Ye, "A standard shielded loop antenna with load resistor," in *Proc. 3rd IEEE Int. Symp. Microw., Antenna, Propag. EMC Technol. Wireless Commun.*, Oct. 2009, pp. 405–407.
- [12] L. L. Libby, "Special aspects of balanced shielded loops," *Proc. IRE*, vol. 34, no. 9, pp. 641–646, Sep. 1946.
- [13] J. Dyson, "Measurement of near fields of antennas and scatterers," *IEEE Trans. Antennas Propag.*, vol. AP-21, no. 4, pp. 446–460, Jul. 1973.
- [14] M. Ishii and K. Komiyama, "Impedance method for a shielded standard loop antenna," *IEEE Trans. Instrum. Meas.*, vol. 56, no. 2, pp. 422–425, Apr. 2007.
- [15] M. Kashanianfard and K. Sarabandi, "An accurate circuit model for input impedance and radiation pattern of two-port loop antennas as E-and H-probe," *IEEE Trans. Antennas Propag.*, vol. 65, no. 1, pp. 114–120, Jan. 2017.
- [16] K. Fujii, Y. Yamanaka, Y. Nakajima, A. Sugiura, and Y. Matsumoto, "A novel standard loop antenna for antenna calibration in the MF and HF bands," in *Proc. IEEE Int. Symp. Electromagn. Compat. (EMC)*, Aug. 2005, pp. 86–89.
- [17] H. Whiteside and R. King, "The loop antenna as a probe," *IEEE Trans. Antennas Propag.*, vol. AP-12, no. 3, pp. 291–297, May 1964.
- [18] A. Boswell, A. J. Tyler, and A. White, "Performance of a small loop antenna in the 3-10 MHz band," *IEEE Antennas Propag. Mag.*, vol. 47, no. 2, pp. 51–56, Apr. 2005.
- [19] T. Miyakawa, K. Nishikawa, and K. Nishida, "An optical-waveguide-type magnetic field probe with a loop antenna element," *Electron. Commun. Jpn. II, Electron.*, vol. 88, no. 4, pp. 18–27, Apr. 2005.
- [20] E. Suzuki, S. Arakawa, H. Ota, K. I. Arai, and R. Sato, "Optical magnetic field probe with a loop antenna element doubly loaded with electrooptic crystals," *IEEE Trans. Electromagn. Compat.*, vol. 46, no. 4, pp. 641–647, Nov. 2004.
- [21] J. E. Lindsay and K. Munter, "Distributed parameter analysis of shielded loops used for wide-band H-Field measurements," *IEEE Trans. Instrum. Meas.*, vol. 32, no. 1, pp. 241–244, Mar. 1983.
- [22] P. Duncan, "Analysis of the Moebius loop magnetic field sensor," *IEEE Trans. Electromagn. Compat.*, vol. EMC-16, no. 2, pp. 83–89, May 1974.
- [23] O. Aluf, "Moebius loop antenna system stability analysis under parameters variation," in *Proc. IEEE Int. Conf. Microw., Antennas, Commun. Electron. Syst. (COMCAS)*, Nov. 2017, pp. 1–5.
- [24] (2018). *FEKO EM Simulation Software*. Altair Engineering. [Online]. Available: <http://www.altair.co.kr>
- [25] M. Ishii and K. Fujii, "Loop antenna calibration methods in low-frequency," in *Proc. Int. Symp. Electromagn. Compat. (EMC/Tokyo)*, May 2014, pp. 290–293.
- [26] M. Ishii and K. Komiyama, "A simple method by measuring the impedance for evaluation of magnetic antenna factor of a loop antenna," *IEICE Electron. Exp.*, vol. 3, no. 5, pp. 92–96, 2006.
- [27] *IEEE Standard Method for Measuring the Shielding Effectiveness of Enclosures and Boxes Having All Dimensions Between 0.1 m and 2 m*, IEEE Standard 299.1-2013, 2014.



magnetic wave propagation, and maritime antennas.

EUNJUNG KANG received the B.S. degree in electronic and electrical engineering from Hongik University, Sejong, South Korea, in 2016. She is currently pursuing the M.S. degree in electronic and electrical engineering with Hongik University, Seoul, South Korea. She was a Research Engineer with the Korea Electronics Technology Institute (KETI), Seongnam, South Korea, from 2016 to 2018. Her research interests include array antenna for wireless power transfer application, electro-



TAE HEUNG LIM received the B.S. and M.S. degrees in electronic and electrical engineering from Hongik University, Seoul, South Korea, in 2016 and 2018, respectively, where he is currently pursuing the Ph.D. degree in electronic and electrical engineering. His research interests include global positioning system antennas, time modulated array, antenna arrays, position optimization of array elements for adaptive beamforming, and wave propagations for radar applications.



SANGWOON YOUN received the B.S. degree in electronic and electrical engineering from Hongik University, Seoul, South Korea, in 2019, where he is currently pursuing the M.S. degree in electronic and electrical engineering. His principal areas of research are EMI and EMC structure and study wave propagation characteristics. His studies include the GPS antennas, direction finding, and anti-jamming systems.

DAE HEON LEE, photograph and biography not available at the time of publication.

KI BAEK KIM, photograph and biography not available at the time of publication.



HOSUNG CHOO (Senior Member, IEEE) received the B.S. degree in radio science and engineering from Hanyang University, Seoul, South Korea, in 1998, and the M.S. and Ph.D. degrees in electrical and computer engineering from the University of Texas at Austin, in 2000 and 2003, respectively. In September 2003, he joined the School of Electronic and Electrical Engineering, Hongik University, Seoul, where he is currently a Professor. His principal areas of research include electrically small antennas for wireless communications, reader and tag antennas for RFID, on-glass and conformal antennas for vehicles and aircraft, and array antennas for GPS applications.

• • •